

# Development of Formulations Based on Acrylate Monomers for Optical Cable Applications

M. C. SENAKE PERERA

School of Science, Griffith University, Nathan, Q 4111, Australia

Received 28 December 2000; accepted 5 April 2001

**ABSTRACT:** Methyl methacrylate and 2-ethyl hexyl acrylate were copolymerized in the presence of different crosslinkers with free-radical initiation. The double-bond conversion was monitored with *in situ* Fourier transform near-infrared spectroscopic techniques. Dynamic mechanical properties of the resultant polymers were measured, and the curves were interpreted on the basis of the heterogeneity and flexibility of the samples. The optical properties of the cables made out of these systems were measured with transmission spectra. The effect of the addition of additives on the optical properties was demonstrated. © 2001 John Wiley & Sons, Inc. *J Appl Polym Sci* 82: 3001–3012, 2001

**Key words:** acrylate; radical polymerization; optical cables; FTIR; dynamic mechanical analysis; copolymerization

## INTRODUCTION

There are many optical applications that require polymers with excellent clarity and mechanical properties. Methyl methacrylate (MMA) and diethylene glycol bis allyl carbonate (CR39) are well-known monomers used in the optical polymer industry and, as a result, their polymerizations and copolymerizations with crosslinking methacrylate monomers have also received extensive attention.<sup>1,2</sup> In addition, many articles have been published recently on the free-radical crosslinking polymerizations of divinyl monomers, and this work has been reviewed by Matsumoto.<sup>3</sup> The free-radical crosslinking copolymerization of styrene and divinyl benzene (DVB) has also received a lot of attention during the last 50 years<sup>4–7</sup> because of the importance of these copolymers in size exclusion chromatography and ion exchange resins.

Use of divinyl monomers in free-radical polymerizations causes crosslinking. When a polymer radical propagates with a double bond of a divinyl monomer, first the unreacted double bond of the same monomer molecule becomes pendant on the chain. If a second polymer radical adds to this double bond, a crosslink forms that ultimately causes gel/network formation. There are several characteristic features<sup>3</sup> of crosslinking polymerizations, including early onset of the Trommsdorff effect and incomplete conversion of double bonds due to vitrification and postpolymerization reactions of trapped radicals with oxygen.

The crosslinking reactions confound the usual diffusion-control nature of free-radical polymerization reactions. As a result, the gel effect (Trommsdorff effect), due to physical entanglements, becomes coupled with the gelation effect of chemical crosslinking. With high levels of divinyl monomer, the autoacceleration can start almost from the very beginning of the reaction. When the three-dimensional network is formed, those reacting species chemically bound to the network, such as pendant double bonds and free-radical centers, have extremely small diffusion coefficients. Con-

Correspondence to: M. C. S. Perera, Mimotopes Pty Ltd., 11 Duerdin Street, Clayton, 3168, Australia (senake\_perera@mimotopes.com).

*Journal of Applied Polymer Science*, Vol. 82, 3001–3012 (2001)  
© 2001 John Wiley & Sons, Inc.

sequently, most of the kinetic parameters may change by several orders of magnitude during the course of the reaction. These rate parameters are the basis for the prediction of the reaction behaviors and polymer chain properties.

The glass-transition temperature ( $T_g$ ) is one of the most important properties exhibited by a polymer, determining its physical state and influencing other properties such as rheological characteristics, mechanical stiffness, and toughness.<sup>8</sup> Below  $T_g$ , the material is brittle, whereas it is ductile, leathery, or liquid above  $T_g$ . The damping properties of a polymer are dominated by its glass transition. When the chain segments in a polymer backbone make de Gennes<sup>9</sup> reptation motions, molecular vibrational energy converts into heat energy, and a loss peak appears in a certain temperature range. Usually, the width of the glass-transition region in a homopolymer is about 20–30°C. There are several methods to increase this transition region width, including polymer blends, interpenetrating networks, and highly crosslinked networks. Similarly, a convenient method to adjust the position of the  $T_g$  according to a given application is to copolymerize monomers A and B in a certain ratio, A/B. The monomers are chosen in such a way that the  $T_g$  values of the two homopolymers lie above and below the required  $T_g$ .

The  $T_g$  of linear polymers as a function of monomer composition and molecular weight are generally well understood.<sup>10</sup> However, the  $T_g$  region of thermoset polymers is not so clearly understood in terms of specific molecular factors. The most common approach is to relate the  $T_g$  of a crosslinked system to the overall conversion,<sup>11</sup> although it is accepted that the variation in  $T_g$  is attributed to various molecular parameters, such as the molecular weight, stiffness, and free volume entrapped in the network.

Currently, optical cables with diameters larger than 5 mm are produced by the partial copolymerization of a mixture of MMA and CR39. The polymerization is terminated<sup>1</sup> at a stage when only 50% CR39 double bonds are reacted. The unreacted double bonds provide flexibility to the cable. However, a drawback of this formulation is that during storage, the CR39 polymerization continues, and the product hardens with time. In this study, copolymers of MMA and 2-ethyl hexyl acrylate (2EHA) were prepared with different crosslinking agents to obtain suitable polymer materials for optical cable applications. The cure profiles, dynamic mechanical properties, and op-

tical properties of the resultant networks are reported in this article. The aim was to find a suitable formulation to give a product with no unreacted monomer but that also had the required hardness, dimensional stability, and optical properties.

## EXPERIMENTAL

### Materials and Sample Preparations

The liquid initiator, *t*-butyl peroxy-2-ethyl hexanoate (TBPEH) was used without any purification. MMA, 2EHA, DVB, hexane diol diacrylate (HDDA), tetra ethylene glycol diacrylate (TEGDA), and tetra propylene glycol diacrylate (TPGDA), CR39 were obtained from Aldrich. DVB, TEGDA, HDDA, TPGDA, and CR39 were used as crosslinkers. The optical additives (OR-B) were obtained from Ciba-Giegy (Australia). The inhibitors of these monomers were removed by passing the liquid monomers through a neutral aluminum column. Mixtures of the initiator and the monomers were made up to the required proportions, and samples of these mixtures were placed in 5-mm glass tubes for Fourier transform near-infrared (FTNIR) spectroscopy. These samples were degassed through three freeze–thaw cycles, after which they were sealed under vacuum. The formulations investigated are given in Table I. Polymerizations were carried out at 60°C with 1% initiator.

### FTNIR Spectroscopy

The FTNIR technique was used to follow the conversion of monomer into polymer because previous workers<sup>12,13</sup> successfully demonstrated the use of this technique to monitor the monomer conversion in polymerization or copolymerization processes. The isothermal polymerizations were monitored *in situ* through measurement of the depletion in the  $\text{>C=CH}_2$  bond peak at  $6132\text{ cm}^{-1}$  for samples placed in a block heater (made in-house) set at the required temperature. The block heater had an entry and exit port for the IR beam, and the temperature of the block was calibrated by insertion of a digital thermocouple directly into an adjacent similar glass tube containing silicon oil. The near-infrared spectra of 16 scans were accumulated every 2 min at a resolution of  $2\text{ cm}^{-1}$  with a PerkinElmer 1600 spectrometer fitted with

**Table I Formulations**

Sample Number	Monomer (wt %)		Crosslinker (wt %)				
	MMA	2EHA	TEGDA	HDDA	DVB	TPGDA	CR39
1	82	13	5				
2	60	35	5				
3	35	60	5				
4	50	50					
5	47.5	47.5	5				
6	45	45	10				
7	40	40	20				
8	60	35		5			
9	45	45			10		
10	40	40			20		
11	35	35			30		
12	60	35				5	
13	45						55

an external bench and mercury cadmium telluride (MCT) detector.

#### Dynamic Mechanical Analysis (DMA)

A PerkinElmer DMA7 instrument was used in the parallel-plate mode on a sample approximately 3 mm wide and 1.5 mm high or in the three-point bending mode on a sample approximately 3 mm in diameter and 15 mm long. Temperature-time scans or stress-strain scans were carried out at a frequency of 1 Hz. A heating rate of 5 K/min was used for the temperature-time scans. Normally, the  $T_g$  value was taken as the point of deflection of the  $\tan \delta$  curve from the base line. However, this was difficult in some samples because of the phase separation and appearance of shoulders in the  $\tan \delta$  peak. As such, the temperature at the maximum point of the  $\tan \delta$  peak was taken as the measure of  $T_g$ . Because the equations used later required  $T_g$  difference values, this was assumed to have no or little error.

#### Measurement of Transmission Spectra

Samples for transmission spectra measurements were prepared by reaction of the mixture of the monomers inside a 10-m fluorinated polymer tube with a water bath. The reaction times determined from Fourier transform infrared (FTIR) measurements were used with suitable modifications to account for increase sample size. After the reaction, the two edges of the tube were cut flat and polished. One edge of the tube was coupled into the light source and the other end to the mono-

chrometer. The wave length of the monochromator was changed manually, the light was allowed to stabilize, and the intensity of the light was measured with a Lux meter.

#### Electron Spin Resonance (ESR)

ESR measurements were carried out with a Bruker ER 200D operating in the X-band frequency range at a modulation frequency of 100 MHz in TE-101 mode. A spectral width of 20 mT was swept over 200 s, which generated 1024 data points, at a modulation amplitude of 2 or 10 dB. Calculation of radical concentration was calibrated with a strong-pitch secondary calibration standard, previously calibrated against a diphenyl picryl hydrazine (DPPH) primary standard. The sample temperature was controlled by a Bruker VT-100 temperature controller/power supply, which was calibrated with the same procedure as for the block heater in the FTNIR.

## RESULTS AND DISCUSSION

It is well known that four types of reactions are involved in a free-radical polymerization, namely; initiation, propagation, termination, and chain transfer. In the case of the bulk free-radical polymerizations of methacrylate monomers, the chain-transfer reaction is negligible. However, it is known that in the polymerization of acrylate monomers, the chain-transfer reaction of the propagating radical to the polymer through a ter-

tiary hydrogen abstraction is significant, especially at high conversion. This leads to crosslink formation. During polymerizations, the polymer chains grow rapidly by the addition of double bonds, and in the presence of a crosslinking agent (monomers with two or more double bonds), this propagation can involve a double bond that is pendant on a preformed polymer chain. The presence of crosslinking monomers in free-radical polymerizations enhances the Trommsdorf effect<sup>14</sup> because of the formation of branched polymer chains and eventually leads to network formation. When a three-dimensional network is formed, the reactive species chemically bound to the network, such as the pendant double bonds and free-radical centers, have extremely small diffusion coefficients, which can significantly suppress their reactivities, even to the extent that they may be considered to be trapped and unavailable for reactions.

Previous studies<sup>15</sup> of polymerizations of dimethacrylates of different chain lengths have shown that an increase in the spacer length between the double bonds increases the polymerization rates, and the final conversions are higher. Dimethacrylate reactions were inhomogeneous, involving microregions of high crosslink density surrounded by regions of low crosslink density.<sup>16</sup> The resultant morphology was a function of the spacer length in the monomer.

In this study, the polymerizations were carried out at 60°C because, through experience, it was noted that the  $T_g$  of the resultant product should be in this temperature range to give the required flexibility. The polymer networks obtained with DVB as the crosslinker in this study was hazy, which indicates a phase separation into two phases with different refractive indices. These had no application in the optical industry, whereas all the other samples prepared in this study gave good transparency.

### Double-Bond Conversion

The conversion–time plots for the monomer mixtures with different proportions of MMA and 2EHA and 5% TEGDA are shown in Figure 1. Autoacceleration occurred at less than 20% conversion. The final extent of cure for isothermal conditions was estimated from the flat portion of the conversion–time curves. The final extent of cure increased with increasing 2EHA content. The addition of 35% 2EHA in the monomer mixture led to complete conversion at a 60°C poly-

merization temperature. With 81% MMA (13% 2EHA), the polymerization did not proceed to full conversion at 60°C. The rate of polymerization also increased with increasing 2EHA content in the monomer mixture.

The double-bond conversion with time for the 50:50 mixture of MMA/2EHA with different amounts of crosslinker, TEGDA, are plotted in Figure 2. Addition of TEGDA had no effect on the polymerization rate in the early stage of the polymerization but reduced the gel point and increased the final conversion. The addition of the crosslinker caused a change in the double-bond concentration in the mixtures, and this can cause a misinterpretation of the results for the polymerization rates. To eliminate the effect of the difference in the double-bond concentrations, the reduced rate ( $R_p/[M]$ ) was calculated and plotted against the conversion in Figure 3.

Because of the higher molecular weight of the crosslinker, its viscosity was higher than that of the monomers. Therefore, the addition of the crosslinker to the monomer mixture increased the viscosity of the mixtures, and this may have reduced the initiator efficiency. However, there was no change in the initial reduced rate of polymerization with the addition of the crosslinker. However, throughout the most of the conversion range, the reduced rate was higher for samples with higher crosslinker contents. However, the long, flexible nature of the crosslinker also introduced more flexibility to the network. Increased flexibility delayed the drop in  $k_p$ , and as a consequence, the monomer reached total conversion. This is confirmed in Figure 4, which shows the conversion–time plots for the same monomer ratio with two different crosslinkers; TEGDA and HDDA. HDDA is a short-length monomer that formed more tight crosslinks. Therefore, additional flexibility was not provided to the system to take to the total conversion.

The use of crosslinker in these formulations was important to achieve the dimensional stability at elevated temperatures. These results show that one could select a combination of MMA/2EHA ratios and type and concentration of crosslinker to prepare polymers without residual monomer at 60°C. Use of long-chain crosslinkers eliminate the risk of residual monomers. However, it is necessary to control the crosslinker concentration to avoid thermal runaway as the reaction rate increases with an increase in crosslinker concentration.

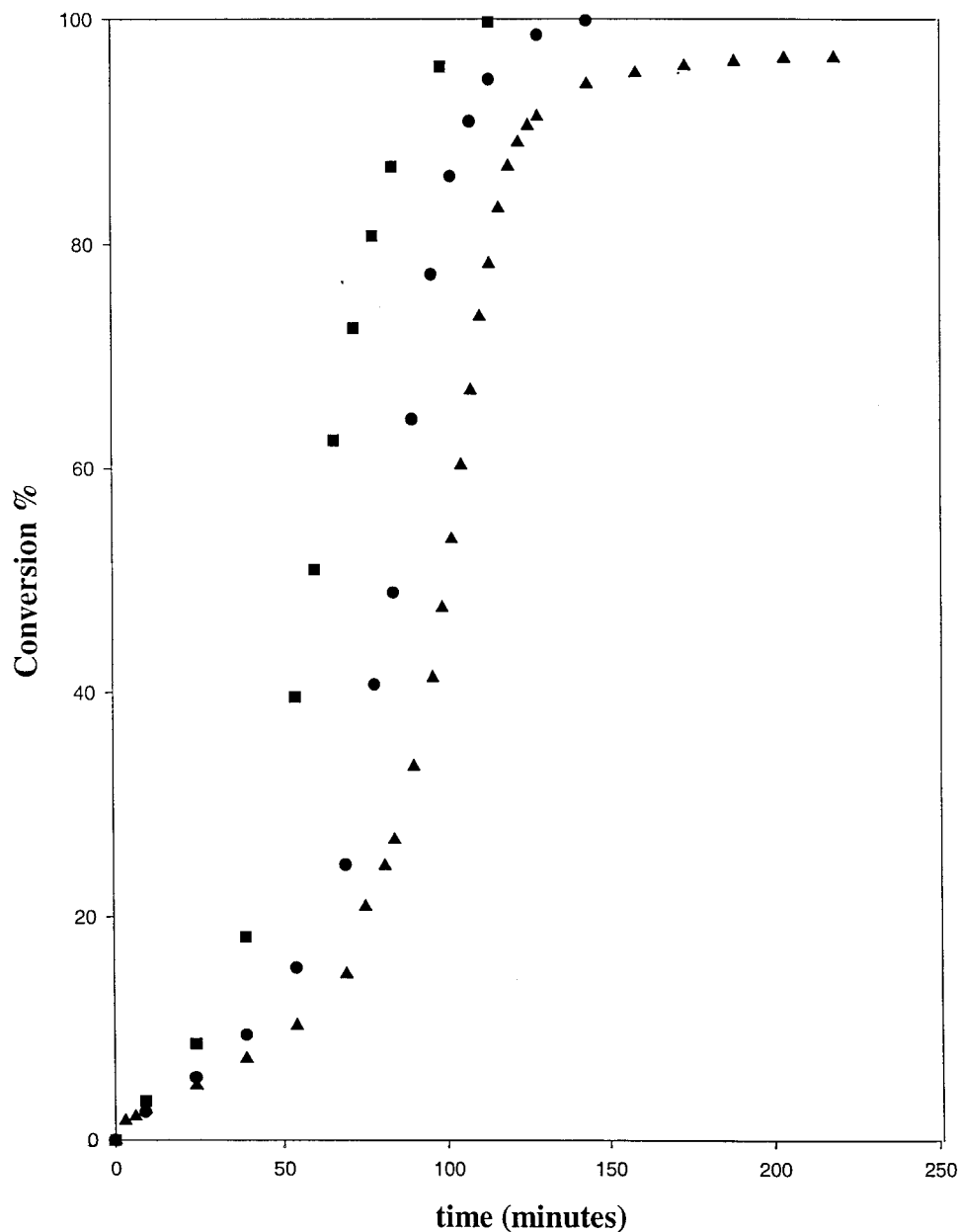


**Figure 1** Monomer conversion with time at 60°C and 1% TBPEH for samples (▲) 1, (●) 2, and (■) 3.

### Dynamic Mechanical Properties

The plots of  $\tan \delta$  versus temperature for polymer matrices prepared with different MMA/2EHA ratios and different crosslinker concentrations are given in Figures 5 and 6. Various parameters derived from the  $\tan \delta$  versus temperature curves are given in Table II. The  $\tan \delta$  plots for all the samples are not shown in the figures so that overlapping is avoided and the figures remain clear. The samples show an increase in the temperature

at the maximum  $\tan \delta$  with increasing MMA content. This was due to the introduction of rigidity to the molecules by the MMA monomer. Interestingly, the width of the  $\tan \delta$  curve for the polymer prepared with the initial 2EHA/MMA ratio of 1.77/3.0 is narrow. However, the deviation of the composition in either direction increases the width of the  $\tan \delta$  curve. Normally, broadening of the curves occur as a result of several factors, including heterogeneity due to crosslinking, the

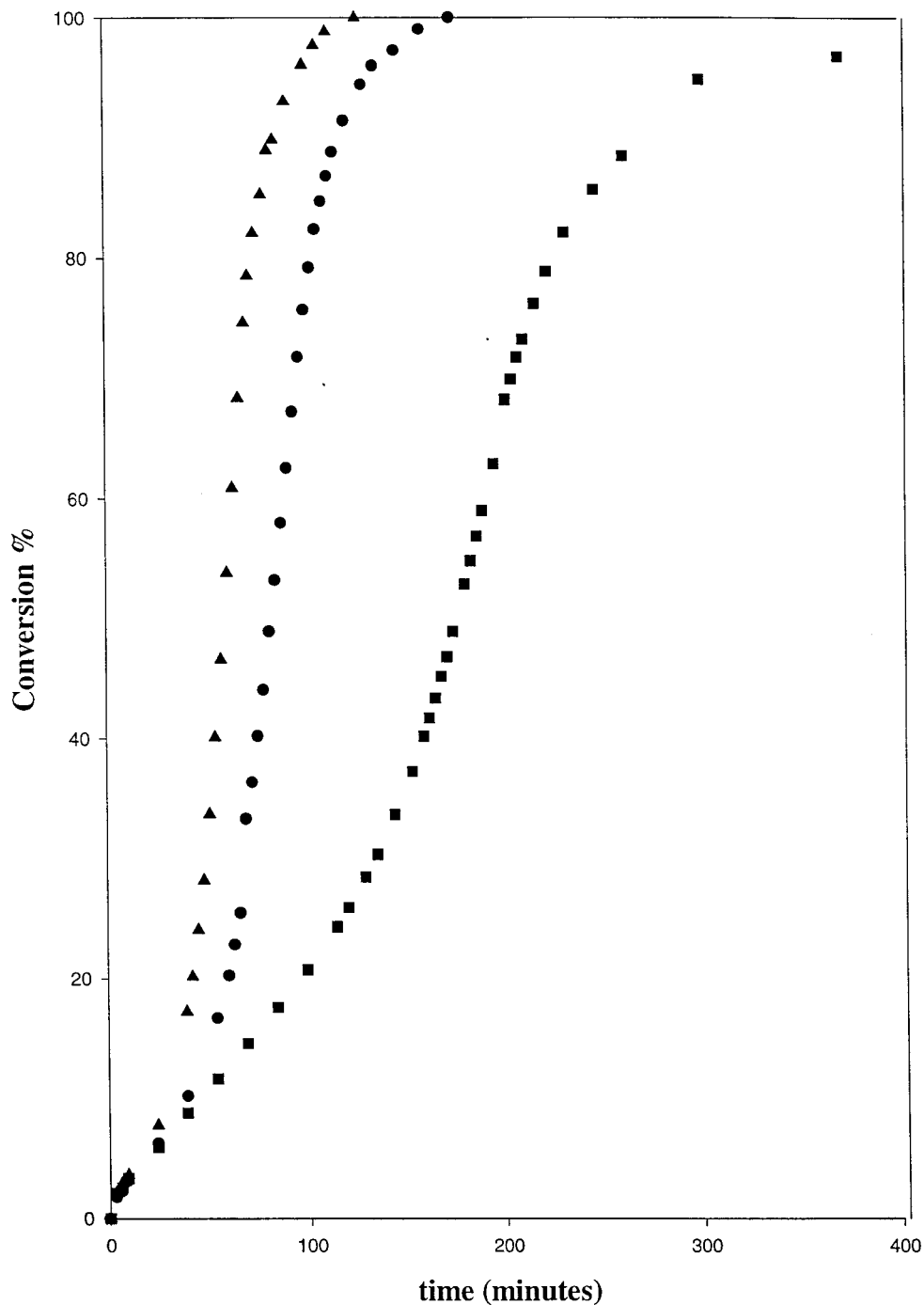


**Figure 2** Monomer conversion with time at 60°C and 1% TBPEH for samples (■) 4, (●) 6, and (▲) 7.

difference in the relative addition of the monomer with time, and microgelation. All these samples were crosslinked with 5% TEGDA; hence, it could not be due to a difference in crosslinking effect. Therefore, the broadening of the  $\tan \delta$  curve may be due to heterogeneity introduced in the system

as a result of the difference in the relative rate of addition (difference in reactivity ratios) of the monomers, or it may be due to microgelation. The faster reaction rate of the sample with a 2EHA/MMA ratio of 3.0/1.77 could have resulted in microgelation in the product. The  $\tan \delta$  curve of the

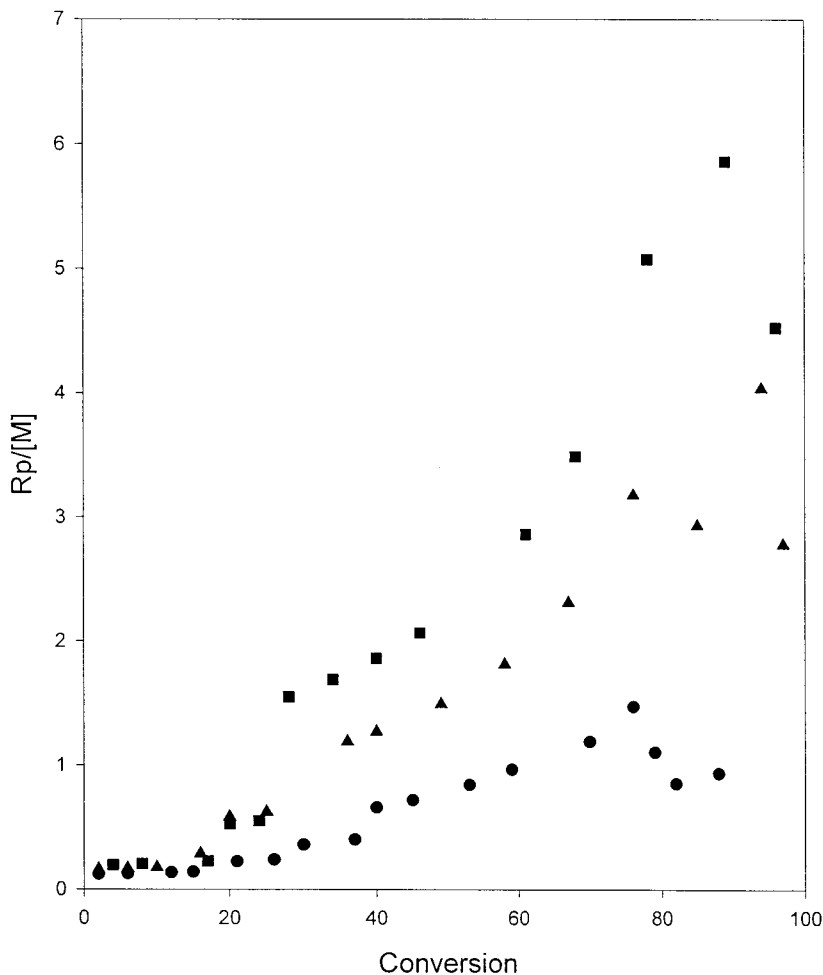


**Figure 3** Reduced rate versus conversion for samples (●) 4, (▲) 6, and (■) 7 at 60°C and 1% TBPEH.

sample with an initial 2EHA/MMA ratio of 0.65/4.1 shows shoulders that indicate heterogeneity and some phase separation. The  $\tan \delta$  maximum temperature of this sample was higher than the reaction temperature, which explains why the polymerization did not go to completion.

As shown in Figure 6, the sample without crosslinker was about 95% converted, whereas the samples with TEGDA crosslinker were fully converted. The  $\tan \delta$  peak for the sample cured without crosslinker is broader than the sample with crosslinker, as shown in Figure 6. Further, the samples with increased TEGDA crosslinker had a lower temperature at  $\tan \delta$  maximum, which indicates that this crosslinker introduced flexibility to the matrix. The introduction of this flexibility was also the reason for the complete conversion in the presence of 5% TEGDA. A similar decrease of the  $T_g$  was also observed when

MMA was copolymerized with the allyl crosslinker, CR39. The temperature at the  $\tan \delta$  maximum for sample 7 was similar to that of sample 3. Sample 7 had higher MMA and TEGDA crosslinker. The two factors had opposing effects. Whereas higher MMA content increased  $T_g$ , TEGDA reduced  $T_g$ . A comparison of the effects of the two crosslinkers HDDA and TEGDA indicated that both crosslinkers gave a network with similar  $T_g$ 's and  $\tan \delta$  curve widths. However, the sample with HDDA was not fully polymerized. DVB gave a network with a higher  $T_g$  and  $\tan \delta$  curve width than the other crosslinkers studied.

The  $\tan \delta$  peaks of the samples of prepared from the 2EHA/MMA ratio of 1/1 with and without crosslinker and the samples prepared from the 2EHA/MMA ratios of 3.0/1.77 and 1.77/3.0 were symmetrical. Symmetrical  $\tan \delta$  curves have been observed in homopolymerized networks of

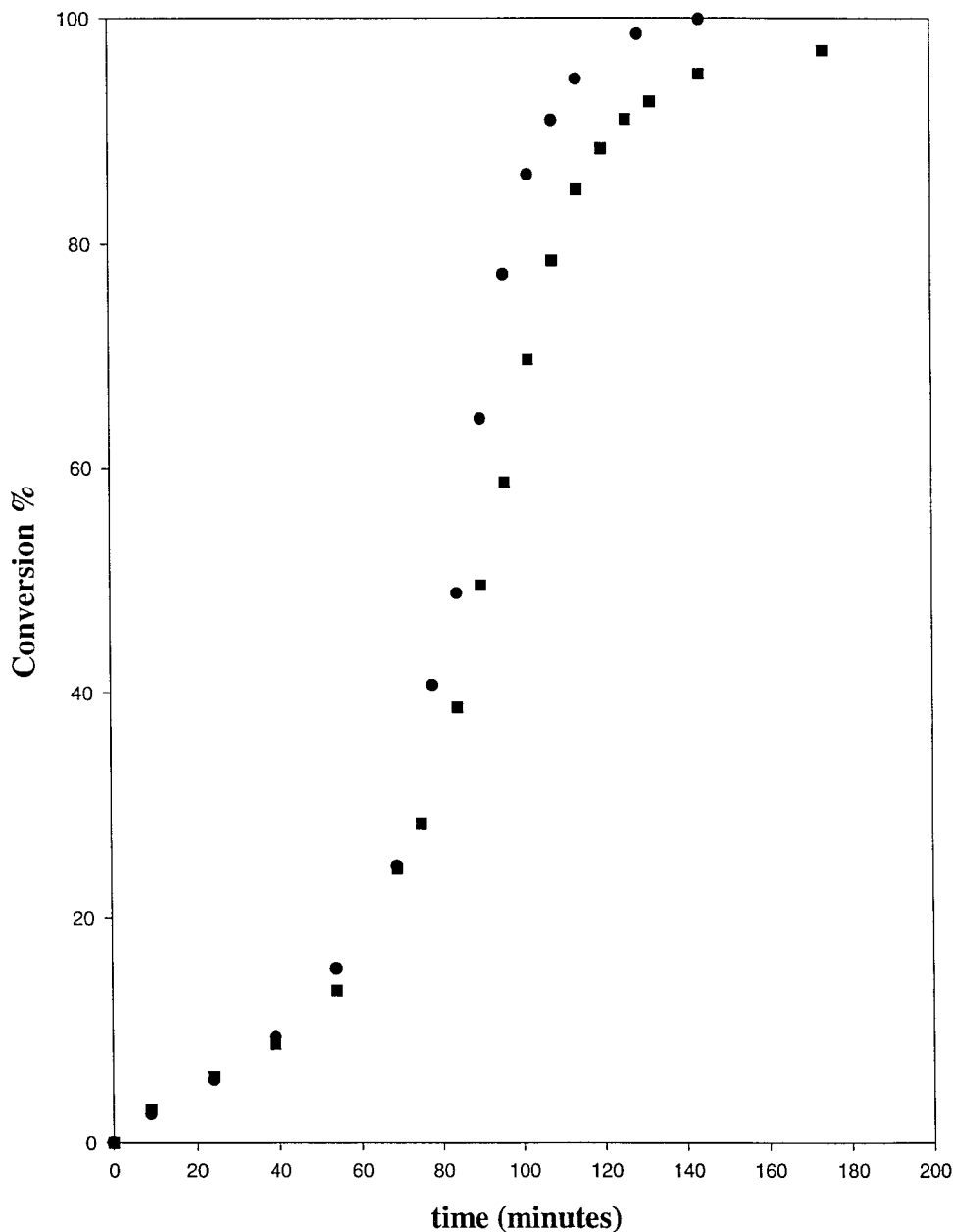


**Figure 4** Monomer conversion with time at 60°C and 1% TBPEH for samples (●) 2 and (■) 8.

other acrylates.<sup>17</sup> We have also observed nonsymmetrical  $\tan \delta$  curves for networks prepared with DVB as the crosslinker.<sup>18</sup> The loss of symmetry in the networks of this study was due to the presence of DVB monomer.

The intensity of the  $\tan \delta$  peak at the  $T_g$  reflects the extent of mobility of the macromolecular chain segments at that temperature.<sup>19</sup> Because crosslinks restrict main-chain mobility in the polymer, one would expect that the area under

the loss modulus curves versus temperature would increase with a decrease in crosslink density. This trend would be reflected in the intensity of the  $\tan \delta$  peak. The  $\tan \delta$  maximum values that correspond to the crosslink density are also given in Table II. The only difference observed was in the presence of DVB crosslinker. The addition of TEGDA had no effect on the  $\tan \delta$  maximum values. The network with tighter crosslink density and correspondingly reduced mobility caused



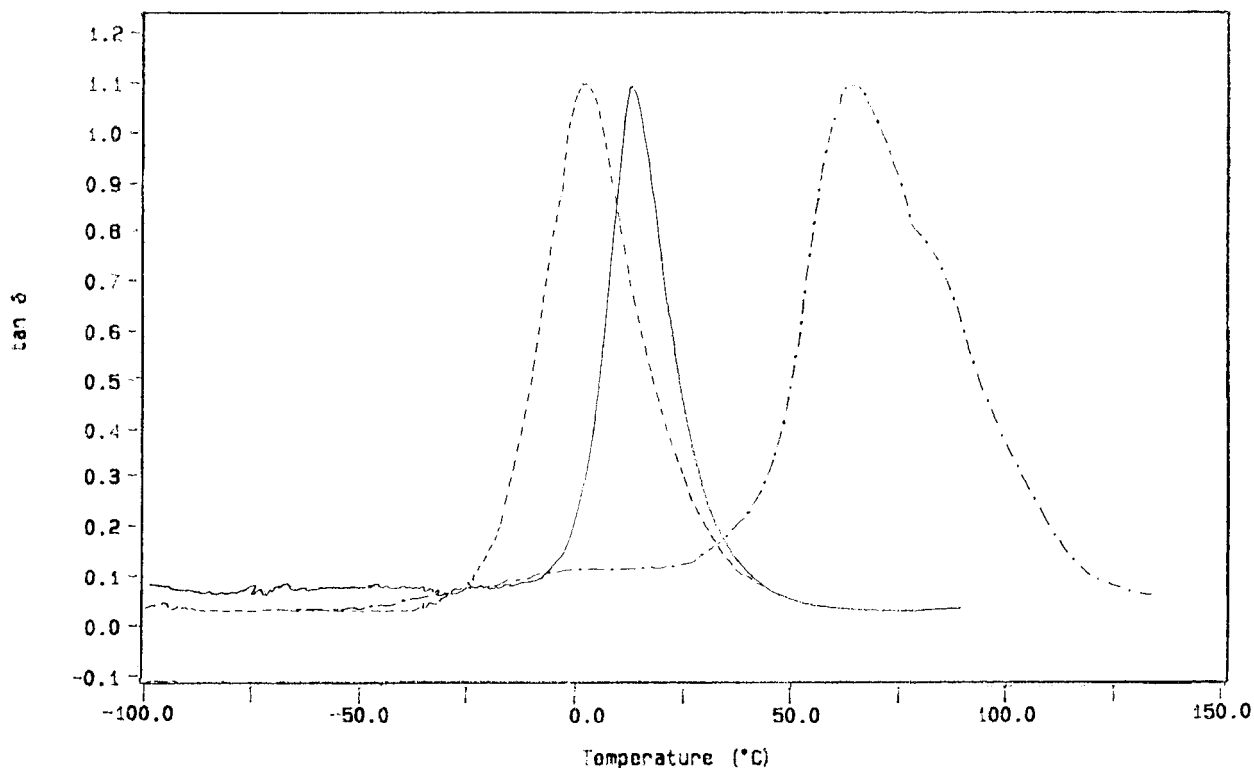


Figure 5 Tan  $\delta$  curves for the cured samples (---) 1, (—) 2, and (-·-) 3.

a reduction in the  $\tan \delta$  maximum value in the network with DVB. Similar effects have been observed in other crosslinking systems;<sup>20</sup> for example, in polypropylene glycol networks, a decrease in  $\tan \delta$  maximum was observed at high crosslink densities, whereas at low crosslink densities, there was virtually no effect on  $\tan \delta$  maximum. In polypropylene glycol, the change in  $\tan \delta$  maximum occurred between  $8 \times 10^{-4}$  and  $2 \times 10^{-2}$  mol/g average molecular weight between crosslinks, and below the value  $8 \times 10^{-4}$  mol/g, there was no change in  $\tan \delta$  maximum.

From the FTIR and DMA data provided so far, the formulation with a 50/50 proportion of the two monomers and 5% TEGDA gave the most suitable product. According to FTIR, there was no residual unsaturation, and DMA indicated minimum heterogeneity. Testing of optical properties were then carried out only on this formulation.

### Optical Properties

One end of the optical cables was coupled to a light source, and the light coming out of the other end was observed. The observed light was slightly yellow in color, and for some applications, whiter

light is preferred. To overcome this problem, the transmission spectra of the cables were measured as described in the Experimental section. The transmission spectrum of a 10-m cable made from the selected formulation is given in Figure 7. The spectrum shows a slight shift toward the yellow region.

An attempt was made to improve the whiteness of the exit light by adding blue pigments to the cable. The pigment was added during the polymerization stage. It was first demonstrated with FTIR that the additives did not effect the polymerization profile. The effect of this blue pigment is demonstrated in Figure 7. There was an overall shift of the spectrum toward the blue region by the addition of the pigment. However, another peak was now visible at about 675 nm. The exit light looked more bluish to the naked eye.

An attempt was made to reduce the yellow coloration by reduction of the initiator concentration. Comparison of the products with different initiator concentrations indicated more yellowing in the sample with lower initiator concentration. The origin of the yellow light was investigated in detail. First, the radical concentration was mea-

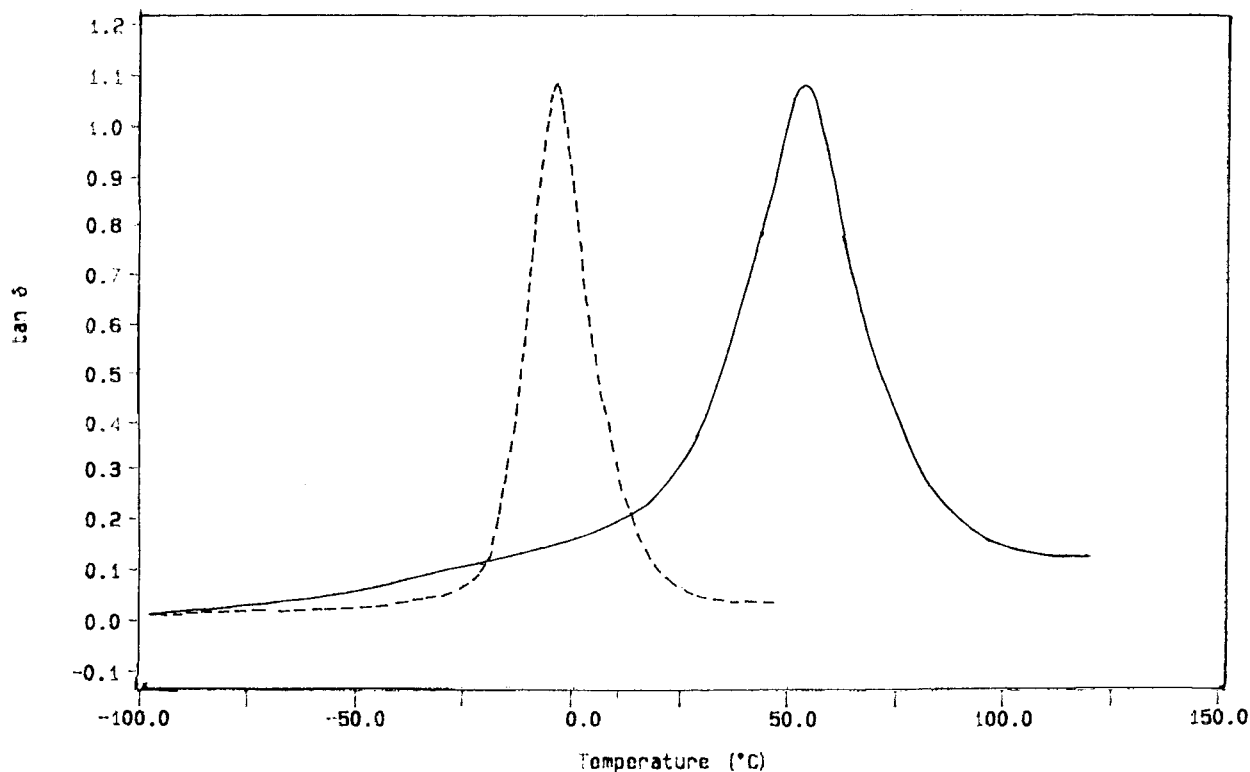


Figure 6 Tan  $\delta$  curves for the cured samples (—) 4 and (---) 7.

sured with time with the ESR technique. The radical concentration with time for the selected formulation is given in Figure 8. It indicates the presence of the residual radicals in the product after polymerization. Trapping of radicals in acrylate and methacrylate polymerization is common. There was a much higher radical concentration in the sample with lower initial initiator concentration. In other words, the final trapped radical concentration was lower with higher initiator concentration. Higher initiator concentration produced much higher radical concentration

at the initial stages of the polymerization, which resulted in an increase in bimolecular termination. This reduced the amount of trapped radicals.

Table II Properties Derived from the DMA Curves

Sample Number	$T_g$ (°C)	Tan $\delta$ Maximum	Half-Width of the Tan $\delta$ Peak (°C)
1	58	1.07	32
2	12.5	1.1	13
3	-5	1.16	20
4	50	1.1	26
5	35	1.1	15
6	-6	1.16	13
7	-6	0.96	13
8	10	1.0	12

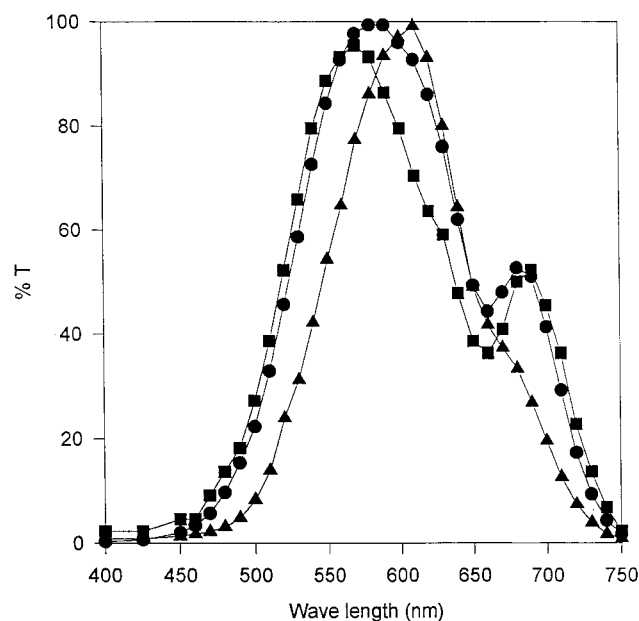
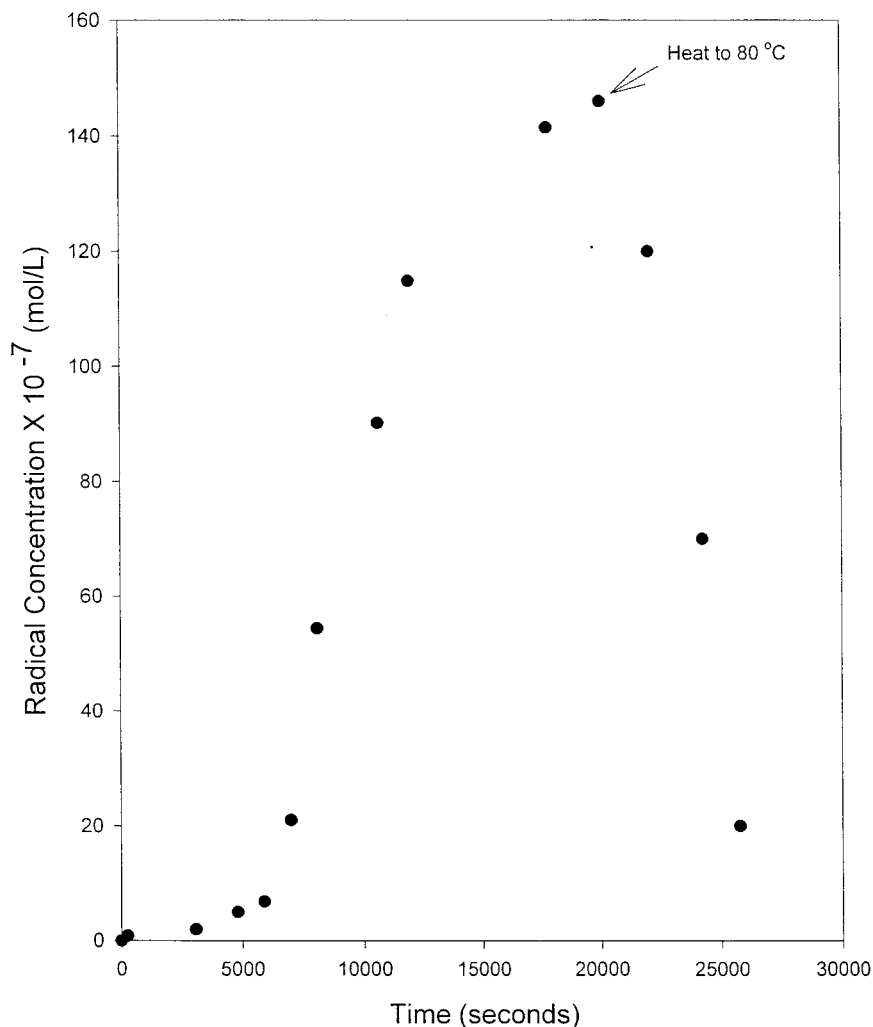


Figure 7 Transmission spectra for sample 5 ( $\blacktriangle$ ) without and with ( $\blacksquare$ )  $1.65 \times 10^{-6}\%$  and ( $\bullet$ )  $2.2 \times 10^{-6}\%$  OR-B additive.



**Figure 8** Radical concentration with time during the curing of sample 5 at 60°C.

The trapped radicals could be removed by heating the product because of the increased molecular mobility. This is also shown in Figure 8. The yellowness of the light decreased with this post-cure treatment.

#### Hardening of the Product with Time

Two-millimeter slices of the optics were cut with a sharp blade and were exposed to ultraviolet (UV) light in a weatherometer. Samples were taken out with time, and their hardnesses were measured with a Shore Durometer Type D and are plotted in Figure 9. The MMA/2EHA/TEGMA sample was compared with the standard product made from the MMA/CR39 formulation. As shown in Figure 9, the MMA/CR39 product hardened with time because of the continuous reaction of the unreacted CR39 double bonds. The addition of UV

stabilizers prevented hardening only for a limited time period. No such hardening was observed in the acrylate product.

#### CONCLUSIONS

The problem of residual monomer in optical cables could be eliminated with a MMA/2EHA/TEGMA formulation. Suitable proportions of the three monomers could be selected to avoid polymerization runaway and to obtain the required flexibility of the cable. *In situ* FTNIR and DMA are suitable techniques for developing the cable formulations. The optical cables produced with these formulations give a slightly yellow light at 10-m lengths. Addition of blue dye to remove this yellowness results in blue light. Use of lower initiator concentrations and postcure treatments

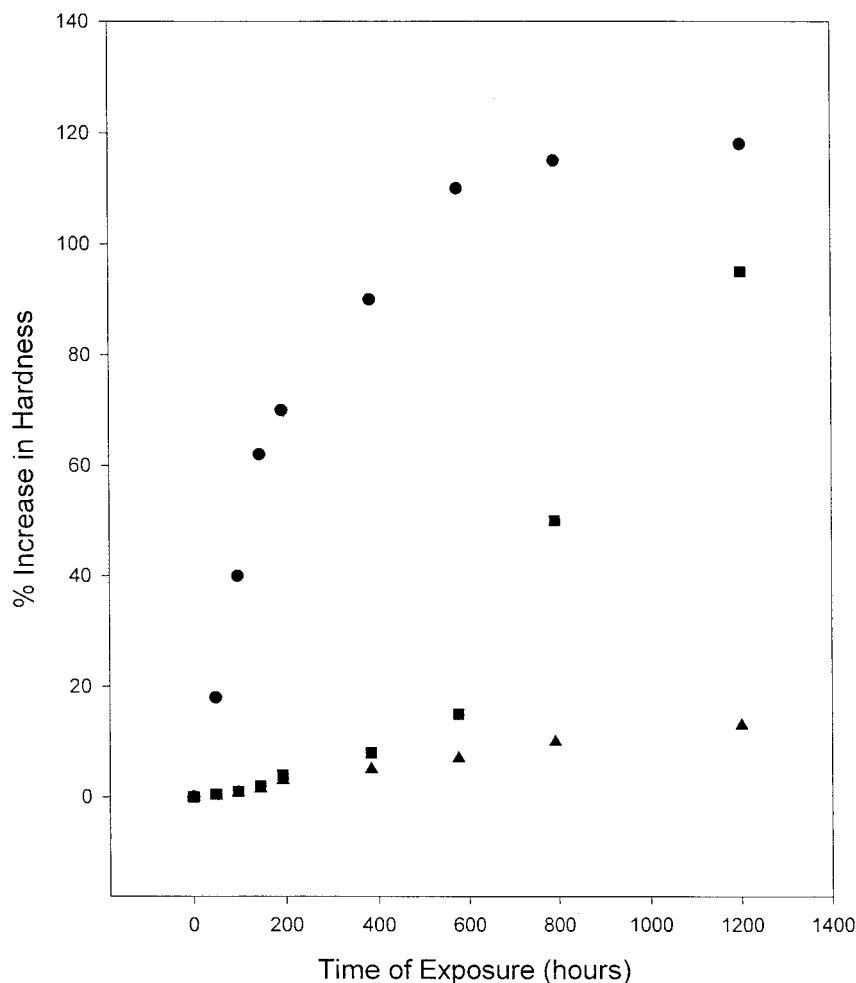


**Figure 9** Percent increase in hardness for (▲) sample 5 and sample 13 (●) without and (■) with the UV stabilizer T 292.

could eliminate the yellowness in the light. There is no hardening of the product with time.

## REFERENCES

- Hill, D. J. T.; O'Donnell, J. H.; Perera, M. C. S.; Pomery, P. J. *Eur Polym J* 1997, 33, 649.
- Zhu, S.; Hamielec, A. *Makromol Chem Macromol Symp* 1992, 63, 135.
- Matsumoto, A. *Adv Polym Sci* 1995, 123, 41.
- Storey, B. T. *J Polym Sci A* 1965, 3, 265.
- Fink, J. K. *J Polym Sci Polym Chem Ed* 1981, 18, 195.
- Hild, G.; Okasha, R. *Makromol Chem* 1985, 186, 93.
- Antoniette, M.; Rosnauer, C. *Macromolecules* 1991, 24, 3434.
- Tobolsky, A. V. *Properties and Structure of Polymers*; Wiley: New York, 1960.
- de Gennes, P. G. *Phys Today* 1983, 36, 33.
- Fox, T. G.; Flory, P. J. *J Polym Sci* 1954, 14, 315.
- Nielson, L. E. *J Macromol Sci Macromol Chem* 1969, 3, 69.
- Hill, D. J. T.; Perera, M. C. S.; Pomery, P. J.; Joseph, E. *Polymer* 1997, 33, 695.
- Hill, D. J. T.; O'Donnell, J. H.; Perera, M. C. S.; Pomery, P. J. *Eur Polym J* 1997, 33, 1353.
- Trommsdorf, V. E.; Kohle, H.; Lagally, P. *Makromol Chem* 1947, 1, 169.
- Allen, P. E. M.; Simon, G. P.; Williams, D. R. G.; Williams, E. H. *Macromolecules* 1989, 22, 809.
- Simon, G. P.; Allen, P. E. M.; Bennet, D.; Williams, D. R. G.; Williams, E. H. *Macromolecules* 1989, 22, 3555.
- Allen, P. E. M.; Clayton, A. B.; Williams, D. R. G. *Eur Polym J* 1994, 30, 427.
- Hill, D. J. T.; Perera, M. C. S.; Pomery, P. J.; Toh, H. K. *Polymer* 2000, 41, 9131.
- Roberts, G. E.; White, E. F. T. In *The Physics of Glassy Polymers*; Hooward, R. N., Ed.; Wiley: New York, 1973; p 53.
- Hsu, C. P.; Lee, J. *Polymer* 1993, 34, 4506.